S1 Detector chamber – InGaAs & InSb setup

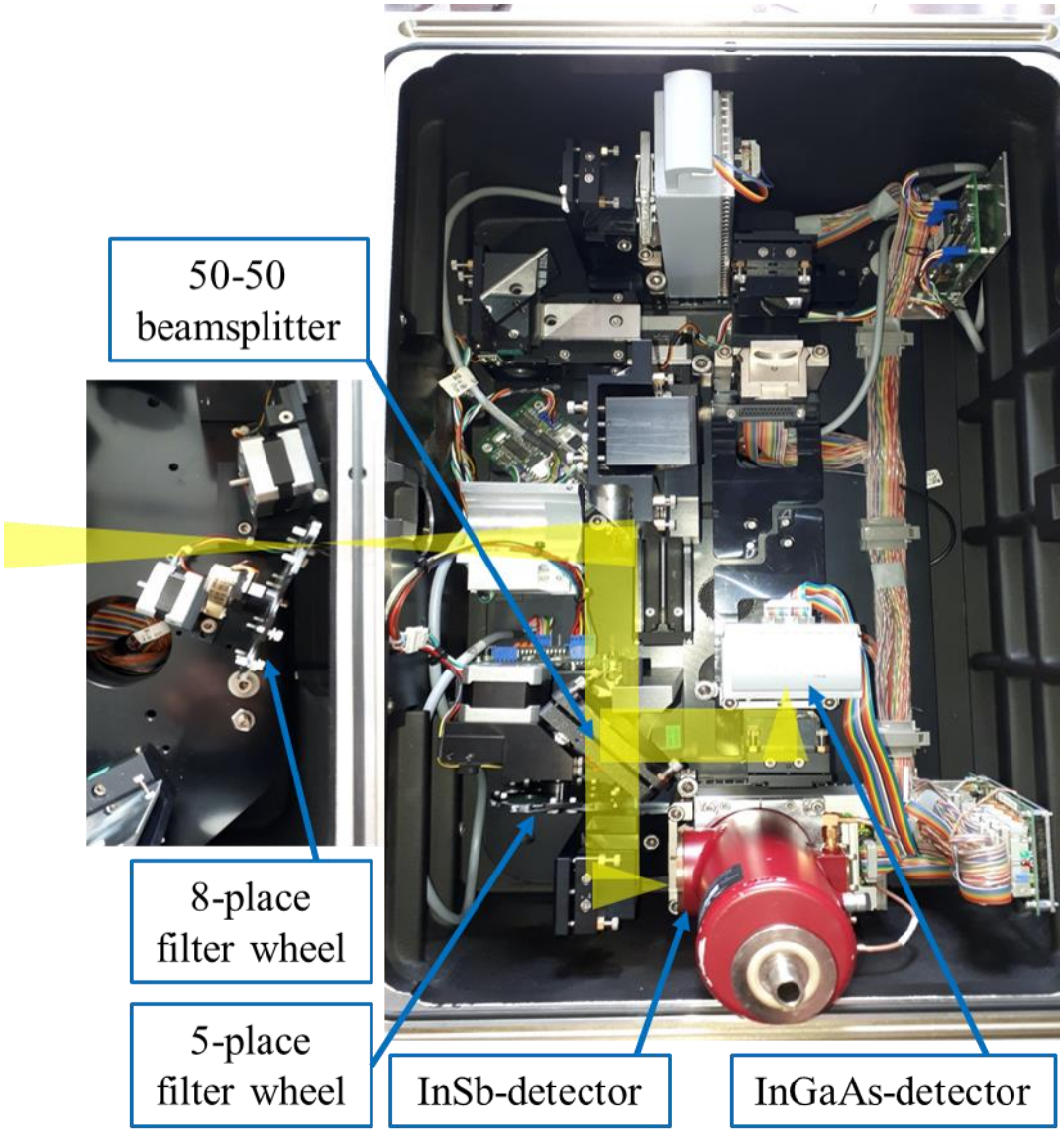

Figure S1: Detector chamber of the FTIR. Yellow path shows the light source entering the chamber, split 50/50 by the CaF_2 beamsplitter (BS) and directed to the InGaAs and InSb detectors. A five-place filter wheel is exchanging the filter in front of the InSb according to the experiment. This five-place filter wheel holds four filters with one place open. An eight-place filter wheel holding two filters, with six open places is located before the detector chamber entrance. The filters' band frequencies (wavenumbers) are presented in Table 1 in the main paper.

S2 The Cyprus AirCores

S2.1 The AirCores sampling

Figure S2: Photos from Nicosia, Cyprus AirCore campaign. A cross section of our AC sampling system (lower left) and the AC just launched (upper left). Here, we use a low-resolution AC device from LSCE built as a double stainless-steel, coated tubing of 35 m long, consisting of a 12 m long 8 mm in diameter tube and a 23 m long 4 mm in diameter tube. The vertical air samples were analysed with a cavity ring-down spectrometry (CRDS) gas analyzer by Picarro, model G2401. Right: photo from the AC launch of 30 June 2020.

Table S1: AirCore flights info

Flight	Date	Launch time (UTC)	Launch location Lat (°N), Lon (°E)	Recovery time (valve closing) (UTC)	Landing location Lat (ºN), Lon (ºE)	Landing location characterization	Balloon cutoff altitude (km)	Profile ceiling (km)	Profile floor (km)	Landing distance from FTS (km)
1	19-6-2020	09:05	35.01, 32.45	11:52	35.11, 33.34	Residential	33	22.86	0.83	5.5
2	29-6-2020	07:46	34.84, 32.87	10:30	35.05, 33.53	Rural	25	21.83	1.43	17
3	30-6-2020	08:40	34.84, 33.39	11:15	34.97, 33.39	Rural	30	23.10	1.11	20

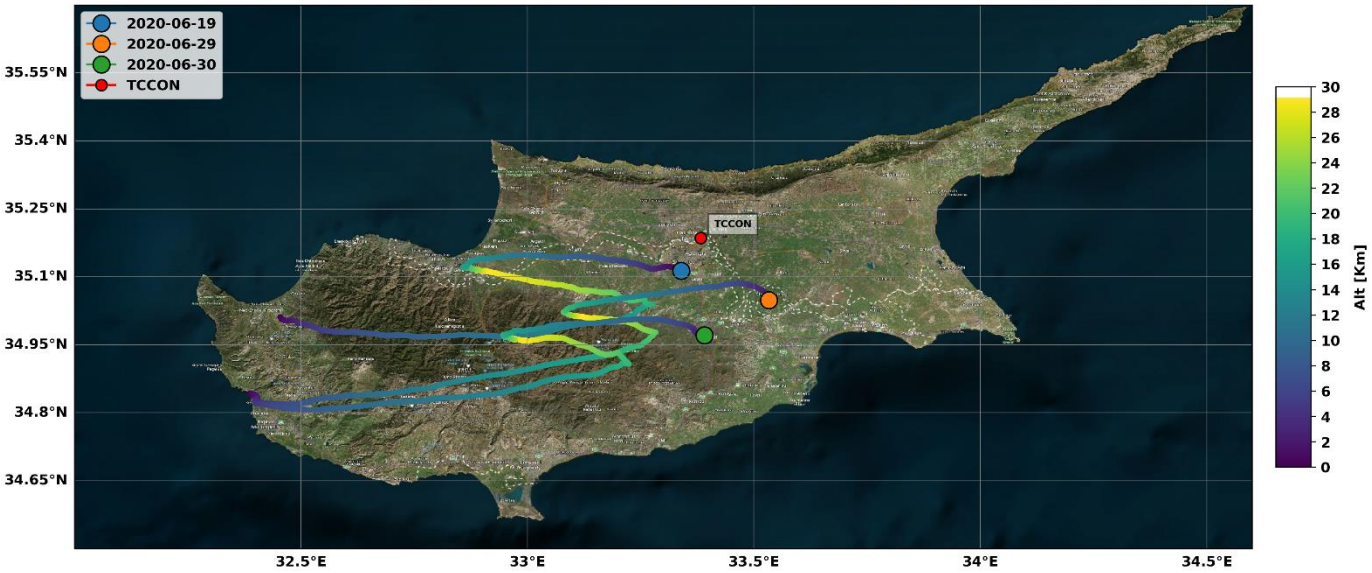

Figure S3: AirCore flights trajectories and landing locations. Map data from © OpenStreetMap contributors 2024. Distributed under the Open Data Commons Open Database License (ODbL) v1.0.

.

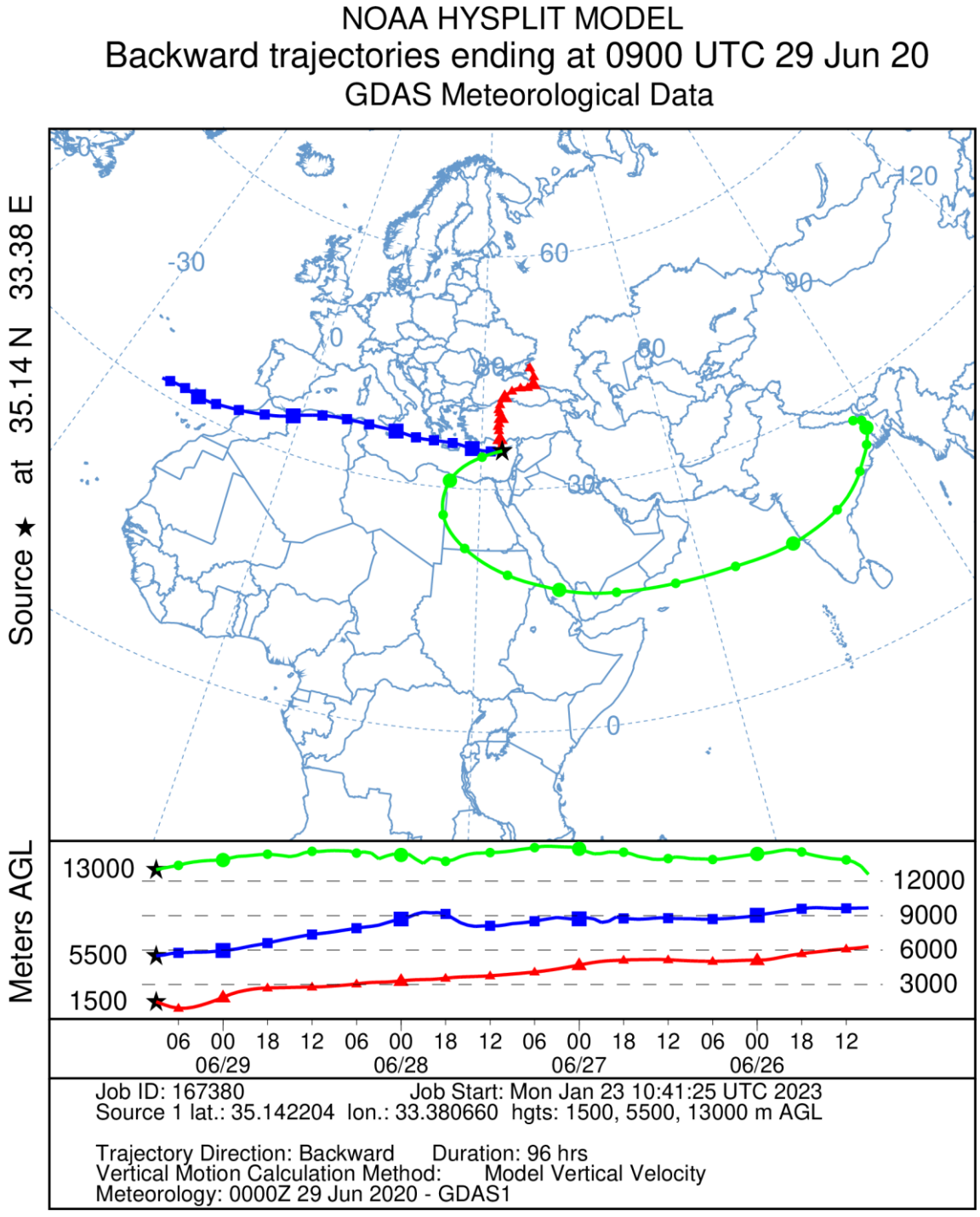

Figure S4: Hysplit airmasses backtrajectories for the AirCore flight of 29 June, running 96 h backwards. Black star represents the location of TCCON Nicosia (Cyprus), where the airmasses (in red, blue and green) arrive on 29 June, at 1.5 km, 5.5 km and 13 km altitude respectively. The green airmass appears to be part of the Asian Summer Monsoon Anticyclone (ASMA), and it was above India 96 h before crossing over Cyprus.

S2.2 FTS Xluft data during AC flights

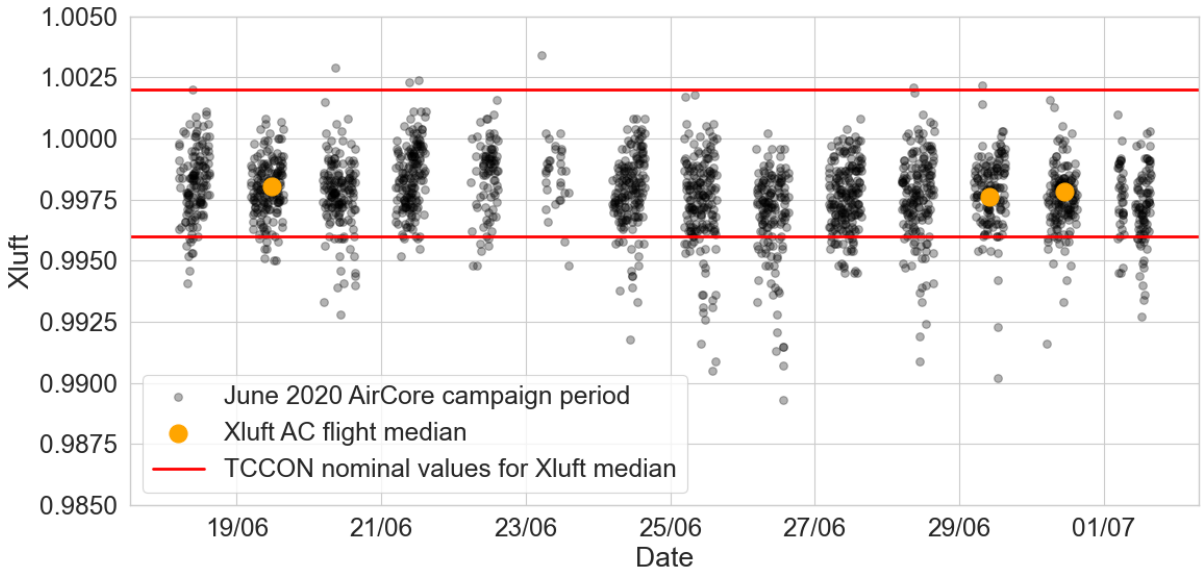

Figure S5: X_{luft} time series during AC campaign (grey markers). X_{luft} flight medians in orange markers and red horizontal lines show the TCCON nominal values for X_{luft} median. This is a check that the X_{luft} flight median is within the median nominal values of 0.996 – 1.002.

S2.3 Constructing the lower and upper bounds of the AirCore profiles

```
# Calculate upper and lower bounds for each species (the AirCore uncertainty)
for specie in species:
    data['lower_alt_unc_lim_' + specie.lower()] = data['lower_alt_unc_lim_' + specie.lower()]/1000 #from m to km
    data['upper_alt_unc_lim_' + specie.lower()] = data['upper_alt_unc_lim_' + specie.lower()]/1000 #from m to km
    data[specie + '_lo'] = data[specie] - unc_values[specie]
    data[specie + '_up'] = data[specie] + unc_values[specie]
    data[specie + '_Alt_min'] = data['Alt'] - data['lower_alt_unc_lim_' + specie.lower()]
    data[specie + '_Alt_max'] = data['Alt'] + data['upper_alt_unc_lim_' + specie.lower()]

    # Calculate bounded means for upper and lower bounds
    data[specie + '_lo_bo'] = data['Alt'].apply(
        lambda x: np.nanmean(data[(x >= data[specie + "_Alt_min"]) & (x <= data["Alt"])][specie + '_lo']))
    data[specie + '_up_bo'] = data['Alt'].apply(
        lambda x: np.nanmean(data[(x <= data[specie + "_Alt_max"]) & (x >= data["Alt"])][specie + '_up']))
```

Figure S6: Python snippet that constructs the lower and upper bounds of the main AirCore. It takes into account the in situ measurement uncertainty per gas specie (unc_values[specie]), which is 0.05 ppm, 0.7 ppb and 7 ppb for CO_2, CH_4 and CO respectively, and the altitude uncertainty limits ('lower_alt_unc_lim_gas_specie' and 'upper_alt_unc_lim_gas_specie'), as provided in the AirCore data files (https://zenodo.org/records/13132338, last access: 5 December 2024) for this type of AC sampling device. For each gas specie, two types for each of lower and upper bounds are constructed. The 'specie_lo' and 'specie_lo_bo' for the lower bounds, and the 'specie_up' and 'specie_up_bo' for the upper bounds. Then, these bounds are treated as extra AirCore profiles. We get the smallest value amongst the 'specie_lo' and 'specie_lo_bo' per altitude to construct the gas lower bound ('gas_lower') and the largest amongst the and 'specie_up' and 'specie_up_bo' to construct the gas upper bound ('gas_upper'). See example in Fig. S7.

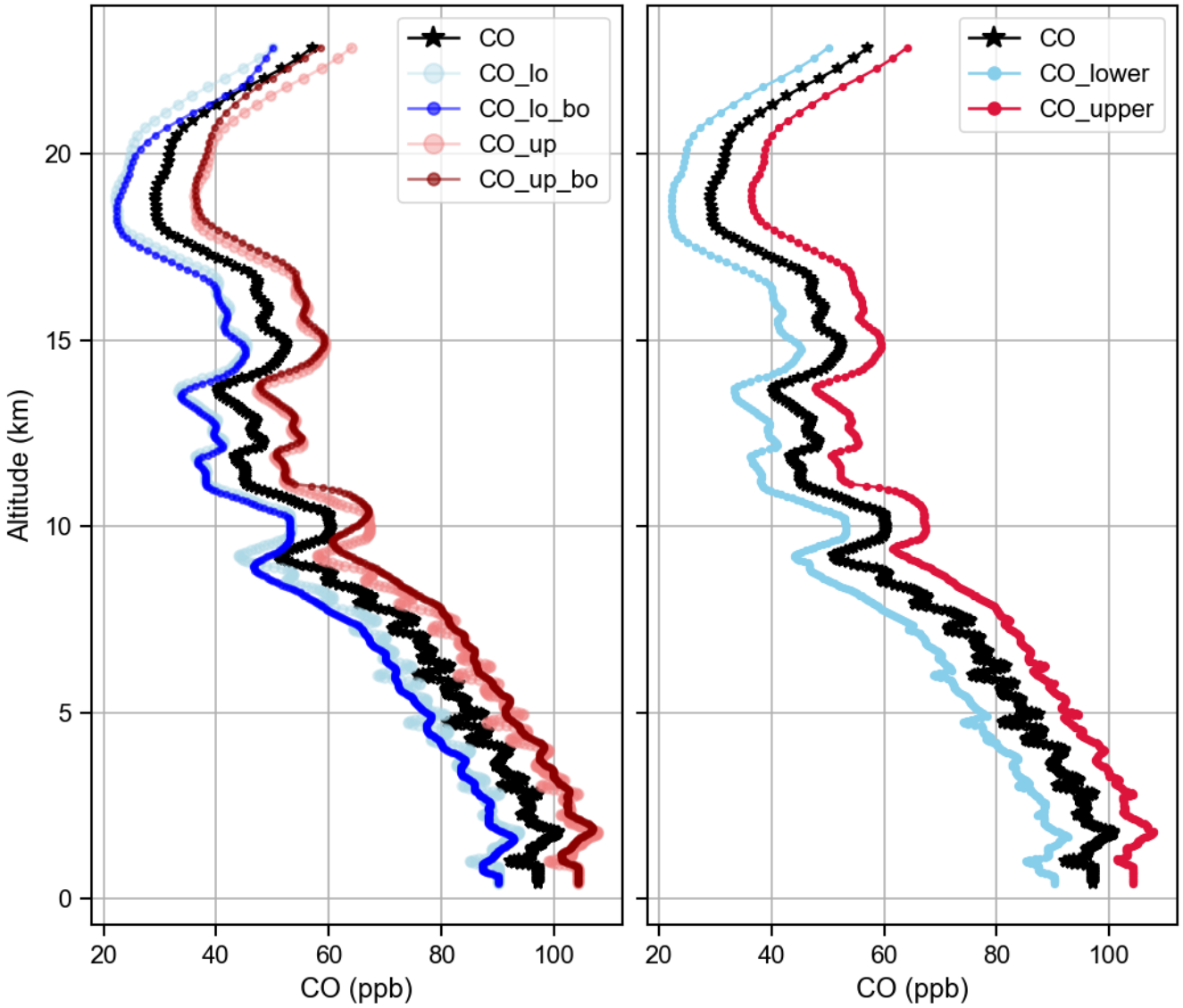

Figure S7: Left: An example of the bounds that result from the python code in Fig. S6 for CO for fight 1. Light blue marker indicates 'specie_lo' and blue marker indicates 'specie_lo_bo'. Pink marker indicates 'specie_up' and dark red indicates 'specie_up_bo'. Right: In order to have just one set of bounds, we selected the smallest value in 'specie_lo' and 'specie_lo_bo' at each altitude to create the gas lower bound ('CO_lower', blue), and similarly, to create the gas upper bound ('CO_upper', red), we selected the largest value in 'specie_up' and 'specie_up_bo' at each altitude.

S2.4 Assembling full profiles

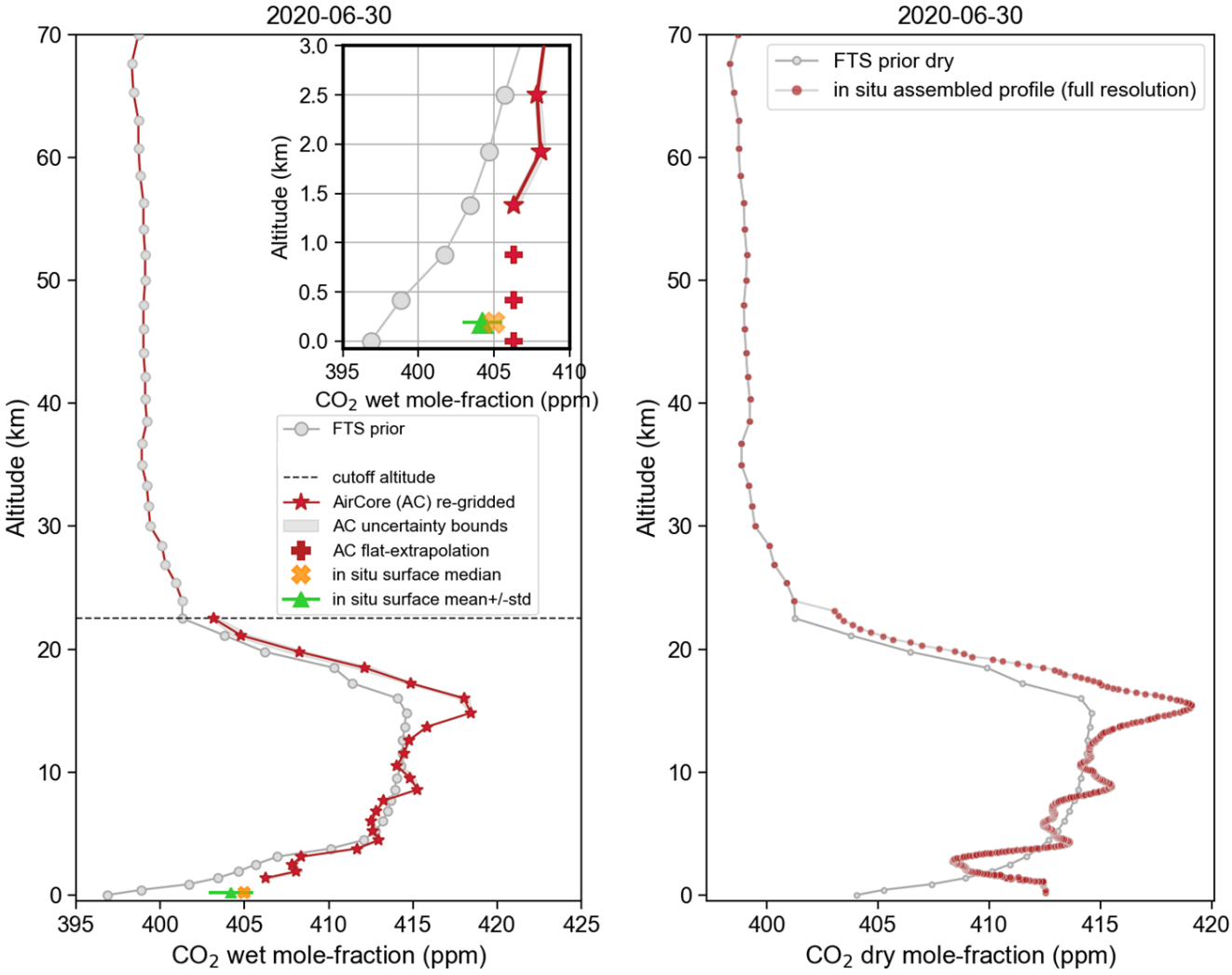

Figure S8: This figure shows a schematic of the approach followed to construct a full vertical profile. For comparability with the FTS prior, the in situ profile needs to extend from 0 m (a.s.l.) to 70 km. Left: Example of an assembled AirCore (AC) profile for the flight on 30 June, 2020, showing CO_2 in wet mole fractions. This vertical resolution profile, was used for the GGG2020 custom retrievals (see Sect. S2.5). Red stars represent the re-gridded AC profile, while a flat extrapolation of the lowest AC measurement to near-ground levels is shown as red crosses in the inset. The grey shading around the main AC profile indicates the uncertainty bounds; which is very small for CO_2. The FTS prior profile is depicted as grey circles connected by a grey line, with the prior used to extend the in situ profile upwards shown as grey circles connected by a red line. The horizontal dashed line marks the altitude of the last AC grid level. Near-surface in situ measurements are represented by the median (orange 'x') and the mean ± standard deviation (green triangle). The inset focuses on the lower 3 km, showing near-surface variability and the comparability between the prior and in situ measurements. A complete profile is constructed by assembling 1) the re-gridded AC profile (red stars), 2) the FTS prior above the highest AC measurement (gray circles with red line), 3) flat extrapolation of the lowest AC measurement to near-ground levels (red cross at 0.88 km), and 4) the in situ surface median (orange 'x') for the lowest two levels (0 and 0.42 km). Right: Assembled AirCore profile in full resolution (in dry mole-fractions). This profile was used as the true profile, x, in Eq. 2, main paper.

S2.5 Running custom GGG2020 retrievals

We follow the method of Laughner et al. (2024) and run custom GGG2020 retrievals by replacing the GGG priors with the assembled AirCore profiles (see Fig. S8, left). Our method of re-gridding the AC profile to the FTS levels is simple (Fig. S8, left), unlike Laughner et al. (2024) that compute weighted averages of the in situ measurements around the adjacent FTS levels (see Sect. C3 and Fig. C1 of Laughner et al. (2024)). Another difference is that when running the GGG2020 custom retrievals, we do apply the in situ correction (AICF) on the custom X_{gas} data as post-processing. In addition, we use retrieved FTS data of spectra recorded within ±1h around the AirCore central flight time instead of the AC landing time.

Table S2 summarizes the retrieval fitting errors of custom versus public data.

Table S2: Measurement errors resulting from the fitting residuals, in "custom" vs. standard data retrievals. Values are rounded to the nearest decimal.

Flight number	**1**	**2**	**3**
	Fitting error mean ± STD		
custom.X_{CO_2} (ppm)	**0.48 ± 0.01**	**0.54 ± 0.01**	**0.57 ± 0.02**
public.X_{CO_2}	**0.45 ± 0.01**	**0.50 ± 0.01**	**0.51 ± 0.01**
custom.X_{CH_4} (ppb)	**2.17 ± 0.04**	**2.20 ± 0.06**	**2.45 ± 0.08**
public.X_{CH_4}	**2.02 ± 0.08**	**2.52 ± 0.06**	**2.33 ± 0.05**
custom.X_{CO} (ppb)	**1.16 ± 0.04**	**0.96 ± 0.01**	**1.13 ± 0.04**
public.X_{CO}	**1.22 ± 0.03**	**0.99 ± 0.02**	**1.13 ± 0.04**

S2.6 X_{gas} and AC.X_{gas} uncertainty calculation

All types of measurements are susceptible to two main types of errors: random and systematic. Below we list error sources for both FTS-derived X_{gas} (valid for standard and custom retrieval) and AirCore (AC)-derived X_{gas} measurements.

[X_{gas}]: The FTS-derived dry-air mole fractions have two known sources of errors described below.

1. Random errors; represented by the measurement variability within the selected flight window of ±1 hour around the AirCore (AC) central time, quantified as the standard deviation around the mean ($\epsilon_{Xgas.std}$).

2. Systematic instrument error; deviations in X_{luft} from the nominal network value (0.999) introduce bias in X_{gas} values. To account for this, we include an X_{luft}-derived bias ($\epsilon_{X_{luft}}$) using Eq. C11 and values in Table C6 from Laughner et al. (2024).

The total uncertainty is calculated by combining standard uncertainties (random errors) in quadrature. Known systematic errors (i.e. $\epsilon_{X_{luft}}$) are added separately, following Eq. 13 in Laughner et al. (2024), here Eq. S1:

$$\epsilon_{X_{gas}} = \sqrt{\epsilon^2_{Xgas.std}} + |\epsilon_{X_{luft}}|, \qquad (S1)$$

Unknown systematic errors are those identified through comparisons with independent measurements, such as WMO-referenced in situ AC profiles. These effects are corrected network-wide using the in situ correction outlined in Sec. 8.3 of Laughner et al. (2024).

[AC.X_{gas}]: For the integrated AC-derived total-column quantity (see Eq. 2, main paper), the primary sources of error arise from:

1. Unmeasured atmospheric sections (Geibel et al., 2012; Laughner et al., 2024; Messerschmidt et al., 2011; Wunch et al., 2010).
2. The AirCore measurements uncertainty.

The magnitude of these uncertainties is largely gas dependent. For point 1) we account for the unmeasured stratospheric and surface levels, and this calculation aims in assessing how the in situ integrated AC.X_{gas} will be affected by the assumptions made to extend it.

Given that our in situ profiles extend up to the lower stratosphere, the most significant unmeasured part is the upper stratosphere. While Messerschmidt et al. (2011) accounted for ~2.02 ppm stratospheric uncertainty for AC.X_{CO_2} by not measuring any part of the stratosphere, our stratospheric uncertainty should be considerably less.

We quantify stratospheric uncertainty (ϵ_{strat}) following Sec. C6 of Laughner et al. (2024), by calculating the difference between a total column-integrated perturbed and unperturbed profile (see Eq. C10 in Laughner et al. (2024)). The perturbed profile is constructed by adding twice the difference between the top AC profile gas value measurement and the corresponding FTS prior level (Eq. C9 in Laughner et al. (2024)). This difference between the AC and the prior value is shown in Fig. S8 (left) at the "cutoff altitude".

For the lowest unmeasured section (typically the lowest 0-1500 m, or 1-3 FTS grid levels), we flat-extrapolate the last AC measurement down to 880 m (the 3rd GGG grid level). From the 880 m to the Nicosia FTS level (180 m) we assume the surface gas value has a range from the surface in situ (Picarro, 185 m ASL) mean ± standard deviation, to the last AC measured value. The total column-uncertainty due to this possible range (ϵ_{ground}) is calculated by integrating profiles where the lowest levels are filled once with the minimum and once with the maximum of this possible range.

AirCore measurements themselves entail uncertainty ($\epsilon_{AirCore}$) arising from the altitude measurement precision, gas mixing during sampling, and instrument precision.

The AC gas and altitude measurement uncertainties provided by LSCE/LMD are used to construct upper and lower profile bounds (see Sect. S2.3). These bounds (see Fig. S7, right) yield the AC uncertainty ($\epsilon_{AirCore}$) when we take the difference between the integrated upper and lower profile bounds, while keeping the unmeasured stratospheric and surface sections appended to the complete profile fixed.

The total error for AC.X_{gas}, incorporating both random ($\epsilon_{AirCore}$, ϵ_{ground}) and systematic (ϵ_{strat}) components, is calculated by Eq. S2 here, following Eq. C12 in Laughner et al., (2024):

$$\epsilon_{AC.X_{gas}} = \sqrt{\epsilon^2_{AirCore} + \epsilon^2_{ground}} + |\epsilon_{strat}|, \quad (S2)$$

Table S3: Uncertainty components for Nicosia retrieved X_{gas} (standard) per gas and per flight. Error sources are the $\epsilon_{Xgas.std}$, representing the measurement variability and $\epsilon_{X_{luft}}$ the X_{luft}-derived bias (see Sec. S2.6). The errors for the custom-retrieved-X_{gas} are not shown as the values are almost identical to the standard retrievals. Values are rounded to the nearest decimal.

Xgas	Flight 1 ϵXgas.std, ϵ-Xluft	Flight 2 ϵ-Xgas.std, ϵ-Xluft	Flight 3 ϵ-Xgas.std, ϵ-Xluft
public.X_{CO_2} (ppm)	0.53, -0.07	0.47, -0.22	0.45, -0.16
public.X_{CH_4} (ppb)	2.2, -0.05	2.1, -0.17	2.5, -0.13
public.X_{CO} (ppb)	1.6, 0	1.2, 0	2.3, 0

Table S4: Uncertainty components for Nicosia AC.Xgas. The ϵ-AirCore component represents the uncertainty in the integrated total column DMF, solely from the AC measurements. Similarly, the ϵ-ground represents the uncertainty in the integrated total column DMF caused by the possible range of values used to fill the near ground profile levels. The ϵ-strat represents the stratospheric error from the unmeasured part of the stratosphere, calculated as described in Sec. S2.6. Last column shows the mean error (± std) of all flights.

AC.X_{gas}	Error source	Flight 1	Flight 2	Flight 3	mean ± std
AC.X_{CO_2} (ppm)	|ϵ-strat| ϵ-ground ϵ-AirCore	0.05 0.02 0.30	0.24 0.20 0.38	0.13 0.02 0.30	0.14 ± 0.10 0.08 ± 0.10 0.33 ± 0.05
AC.X_{CH_4} (ppb)		10.1 0.1 10.2	9.5 0.3 7.5	1.9 0.5 7.7	7.2 ± 4.6 0.3 ± 0.2 8.5 ± 1.5
AC.X_{CO} (ppb)		1.8 0.3 15.3	5.6 0.3 15.1	3.7 1.2 15.8	3.7 ± 1.9 0.6 ± 0.5 15.4 ± 0.3

References

Geibel, M. C., Messerschmidt, J., Gerbig, C., Blumenstock, T., Chen, H., Hase, F., Kolle, O., Lavrič, J. V., Notholt, J., Palm, M., Rettinger, M., Schmidt, M., Sussmann, R., Warneke, T., and Feist, D. G.: Calibration of column-averaged CH_4 over European TCCON FTS sites with airborne in-situ measurements, Atmos. Chem. Phys., 12, 8763–8775, https://doi.org/10.5194/acp-12-8763-2012, 2012.

Laughner, J. L., Toon, G. C., Mendonca, J., Petri, C., Roche, S., Wunch, D., Blavier, J.-F., Griffith, D. W. T., Heikkinen, P., Keeling, R. F., Kiel, M., Kivi, R., Roehl, C. M., Stephens, B. B., Baier, B. C., Chen, H., Choi, Y., Deutscher, N. M., DiGangi, J. P., Gross, J., Herkommer, B., Jeseck, P., Laemmel, T., Lan, X., McGee, E., McKain, K., Miller, J., Morino, I., Notholt, J., Ohyama, H., Pollard, D. F., Rettinger, M., Riris, H., Rousogenous, C., Sha, M. K., Shiomi, K., Strong, K., Sussmann, R., Té, Y., Velazco, V. A., Wofsy, S. C., Zhou, M., and Wennberg, P. O.: The Total Carbon Column Observing Network's GGG2020 data version, Earth Syst. Sci. Data, 16, 2197–2260, https://doi.org/10.5194/essd-16-2197-2024, 2024.

Messerschmidt, J., Geibel, M. C., Blumenstock, T., Chen, H., Deutscher, N. M., Engel, A., Feist, D. G., Gerbig, C., Gisi, M., Hase, F., Katrynski, K., Kolle, O., Lavrič, J. V., Notholt, J., Palm, M., Ramonet, M., Rettinger, M., Schmidt, M., Sussmann, R., Toon, G. C., Truong, F., Warneke, T., Wennberg, P. O., Wunch, D., and Xueref-Remy, I.: Calibration of TCCON column-averaged CO_2: the first aircraft campaign over European TCCON sites, Atmos. Chem. Phys., 11, 10765–10777, https://doi.org/10.5194/acp-11-10765-2011, 2011.

Wunch, D., Toon, G. C., Wennberg, P. O., Wofsy, S. C., Stephens, B. B., Fischer, M. L., Uchino, O., Abshire, J. B., Bernath, P., Biraud, S. C., Blavier, J.-F. L., Boone, C., Bowman, K. P., Browell, E. V., Campos, T., Connor, B. J., Daube, B. C., Deutscher, N. M., Diao, M., Elkins, J. W., Gerbig, C., Gottlieb, E., Griffith, D. W. T., Hurst, D. F., Jiménez, R., Keppel-Aleks, G., Kort, E. A., Macatangay, R., Machida, T., Matsueda, H., Moore, F., Morino, I., Park, S., Robinson, J., Roehl, C. M., Sawa, Y., Sherlock, V., Sweeney, C., Tanaka, T., and Zondlo, M. A.: Calibration of the Total Carbon Column Observing Network using aircraft profile data, Atmos. Meas. Tech., 3, 1351–1362, https://doi.org/10.5194/amt-3-1351-2010, 2010.